

Supporting Information

Hollow anisotropic semiconductor nanoprisms with highly crystalline frameworks for high-efficiency photoelectrochemical water splitting

Erhuan Zhang,^a Jia Liu,^{a} Muwei Ji,^b Hongzhi Wang,^a Xiaodong Wan,^a Hongpan Rong,^a Wenxing Chen,^a Jiajia Liu,^a Meng Xu,^a and Jiatao Zhang^{a*}*

^a Beijing Key Laboratory of Construction Tailorable Advanced Functional Materials and Green Applications, Experimental Center of Advanced Materials, School of Materials Science and Engineering, Beijing Institute of Technology, Beijing 100081, PR China

^b Graduate School at Shenzhen, Tsinghua University, Shenzhen, 518055, P.R. China

-

Experimental Section

Synthesis of Ag nanoprisms. The synthesis of Ag triangular nanoprisms was performed in a hydrothermal autoclave reactor according to the method reported previously.¹ A mixture containing 25 mL of DMF and 50 mM of PVP was prepared in the autoclave (40 mL) at room temperature, and then 1 mM of AgNO₃ was added. The obtained uniform dark brown solution was sealed and heated at 150 °C for 12 h. The sample was washed by ethanol three times and re-dispersed in ultrapure water.

Sulfuration reaction. The Na₂S_x aqueous solution was prepared by reacting Na₂S aqueous solution with sulfur powders as reported by Xia et al.² In a typical process, 32 mg of sulfur powders were mixed with 11.7 mL of Na₂S aqueous solution (50 mM) in a vial (15 mL). The suspension was agitated sonication for about 4 hours. The vial was then sealed and placed in an oven at 80 °C for 12 h. The color of the solution turned to bright yellow once the sulfur powders were completely dissolved. The concentration of sulfur was around 135.4 mM in the final solution. For sulfuration procedure, typically, 0.2 mL of the prepared Na₂S_x aqueous solution was added to 30 mL of the aqueous suspension of Ag triangular nanoprisms (1.0 mM in terms of elemental silver) at room temperature under magnetic stirring. After desired time durations, the reaction was quenched by centrifugation at 8000 rpm for 6 min. The resultant Ag@Ag₂S core-shell nanoprisms were then precipitated twice with water by centrifugation, and re-dispersed in ultrapure water.

Cation exchange and its induced oxidative etching. To synthesize Ag@CdS core-shell nanoprisms, the obtained Ag@Ag₂S core-shell nanoprisms were re-dispersed in CTAB aqueous solution (10 mL, 50 mM), and then mixed with Cd(NO₃)₂·4H₂O aqueous solution (1.5 mL, 0.05 g mL⁻¹) as well as 5 μL of TBP (dissolved in a minor amount of methanol). The resulting mixture was heated to 60 °C in a water bath and kept at this temperature for 2 h. As for the Ag@CdS partially-hollow nanoprisms and hollow CdS nanoprisms, similar procedures were conducted except that the amount of TBP used for initiating cation exchange was increased (10 μL - 30 μL for Ag@CdS partially-hollow nanoprisms and 40 μL for hollow CdS nanoprisms). The resulting samples were washed, collected by centrifugation and re-dispersed in pure water. The synthesis of Ag@ZnS core-shell nanoprisms, Ag@ZnS partially-hollow nanoprisms and hollow ZnS nanoprisms was performed resembling the Ag@CdS core-shell nanoprisms, Ag@CdS partially-hollow nanoprisms and hollow CdS nanoprisms, correspondingly, except that the Cd(NO₃)₂·4H₂O was replaced with Zn(NO₃)₂·6H₂O during the cation exchange step.

Characterizations: Low-resolution transmission electron microscopy (TEM) images were obtained by HITACHI H-7650 (accelerating voltage of 80 kV) electron microscopy. High-resolution transmission electron microscopy (HRTEM) characterization and energy dispersive X-ray spectroscopy (EDS) analysis were performed using transmission electron microscopy (FEI Tecnai G2 F20 S-Twin, acceleration voltage of 200 kV) equipped with X-ray energy-dispersive spectroscopy detector. The powder X-ray diffraction measurements were performed using a Bruker D8 multiply crystals X-ray diffractometer (5° per min). The UV-Vis-NIR measurements were carried out on a Shimadzu UV3600 UV-Vis spectrophotometer at room temperature. The X-ray photoelectron spectroscopy (XPS) analysis was performed on a PerkinElmer Physics PHI 5300 spectrometer.

Photoelectrochemical (PEC) measurements and hydrogen evolution: The PEC measurements were performed using a standard three-electrode potentiostat system on Instruments760D electrochemical workstation (Chenghua, Shanghai, China) with a working electrode, a Pt counter electrode, and a Ag/AgCl reference electrode. The working electrode was prepared by depositing active films of the sample on the FTO substrate (1 cm × 2 cm) that has been previously cleaned with ethanol and water. The surface area of the sample exposed to the electrolyte was fixed at 1 cm². An aqueous solution containing 0.5 M of Na₂S and 0.5 M of Na₂SO₃ (pH of ~13.6) was used as the electrolyte to maintain the stability of the sulfide electrodes.^{3,4} The working electrode was illuminated from the front side with a 300 W Xe lamp (FX300, Beijing Perfectlight Technology) equipped with an AM 1.5 solar simulation filter (100 mW cm⁻²). The *I*-*V* and *I*-*t* (at a fixed bias potential of -0.4 V versus Ag/AgCl) curves were measured under chopped light irradiation. The EIS Nyquist plots were collected with the frequency ranging from 100 kHz to 0.01 Hz and the modulation amplitude of 5 mV. The PEC hydrogen evolution experiments were performed in a Pyrex reaction cell connected to a closed gas circulation and evacuation system (Labsolar 6A, Beijing Perfectlight Technology) under the same conditions as for the photocurrent measurements. The reaction cell was maintained at 25 °C by a flow of cooling water bath during the reaction. The amount of evolved H₂ was analyzed by a gas chromatograph (Agilent 7890B GC system) equipped with a thermal conductivity detector (TCD) and a molecular sieve 5A column. IPCE can be calculated using the following equation,

$$IPCE = (1240 \times I) / (\lambda \times J) \times 100\%$$

where λ is the wavelength of the incident light, I is the measured photocurrent density at the specific wavelength, and J is the measured power intensity of the incident light at the specific wavelength.

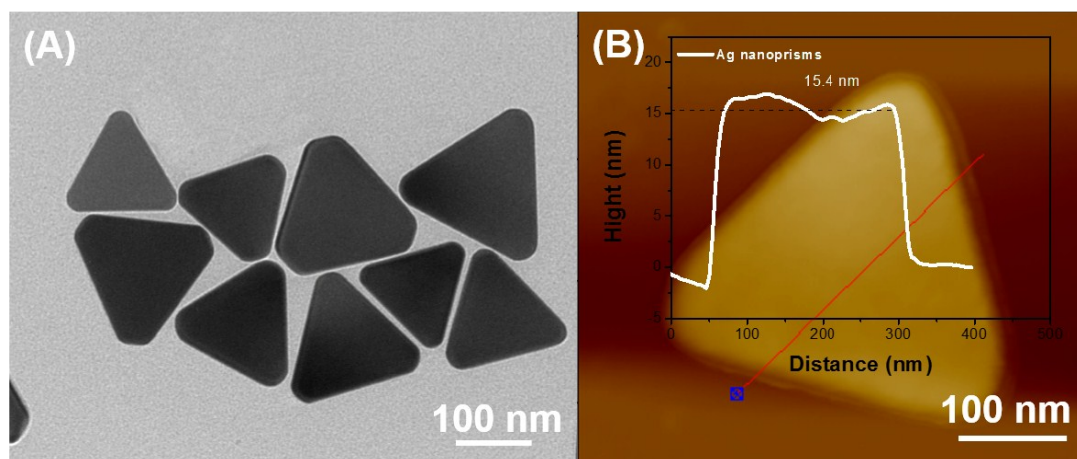


Fig. S1. (A) TEM image and (B) AFM image of Ag triangular nanoprisms.

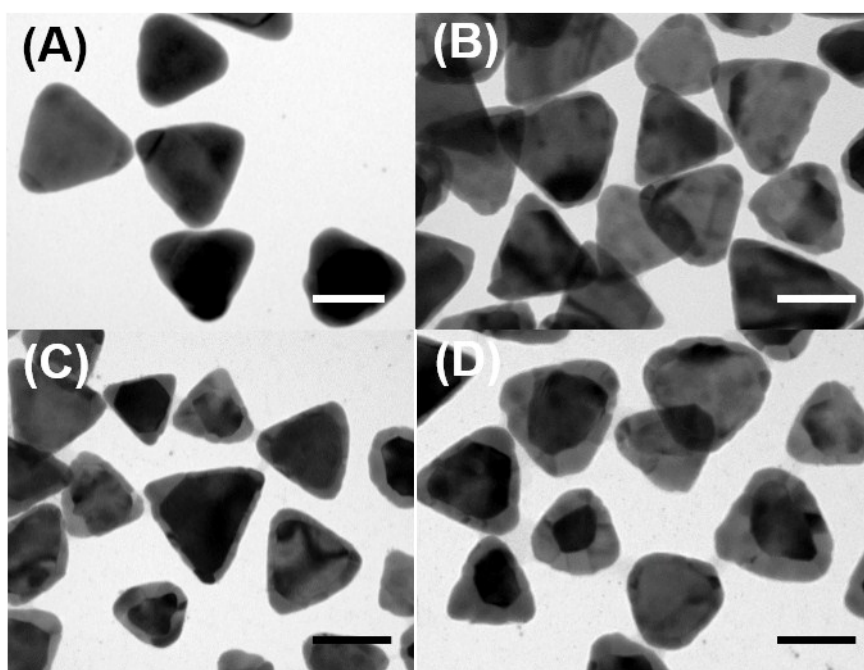


Fig. S2. Control over the sulfuration degree of Ag triangular nanoprisms to obtain Ag@Ag₂S hybrid nanoprisms with different area of Ag₂S regions. The addition amount of Na₂S_x and reaction time are (A) 100 μ L of Na₂S_x, 15 s, (B) 100 μ L of Na₂S_x, 1 min, (C) 200 μ L of Na₂S_x, 5 min, and (D) 300 μ L of Na₂S_x, 5 min, respectively. Scale bar is 100 nm.

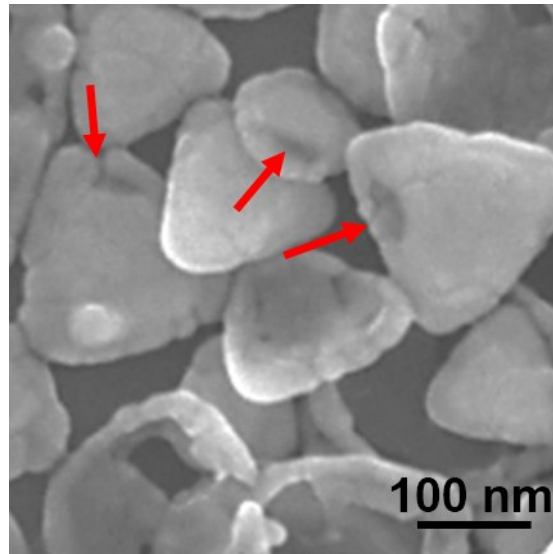


Fig. S3. SEM image of hollow CdS nanoprisms. The red arrows indicate the hollow cavity inside the nanoprisms.

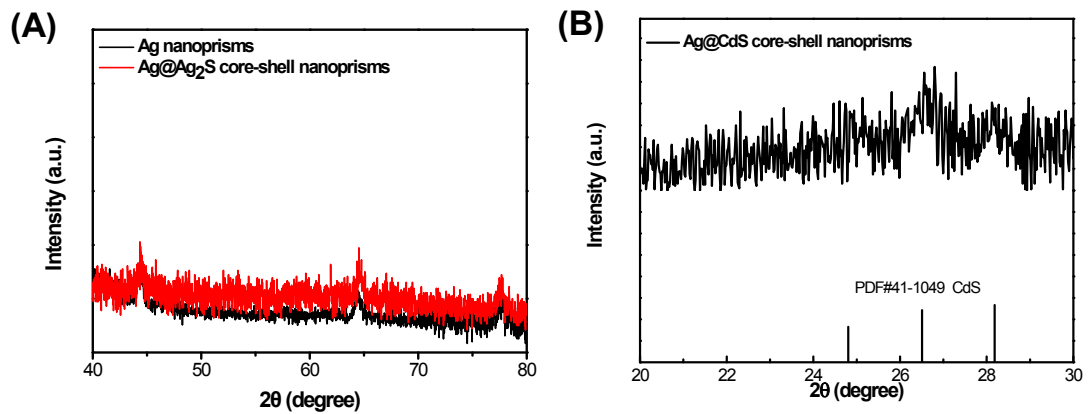


Fig. S4. Detailed analysis of the XRD patterns. (A) The magnified XRD patterns of Ag nanoprisms and Ag@Ag₂S core-shell nanoprisms show the diffraction peaks assigned to the (200), (220) and (311) facets of fcc Ag, respectively. (B) The magnified XRD pattern of Ag@CdS core-shell nanoprisms shows three characteristic diffraction peaks assigned to (100), (002) and (101) facets of hexagonal CdS, respectively.

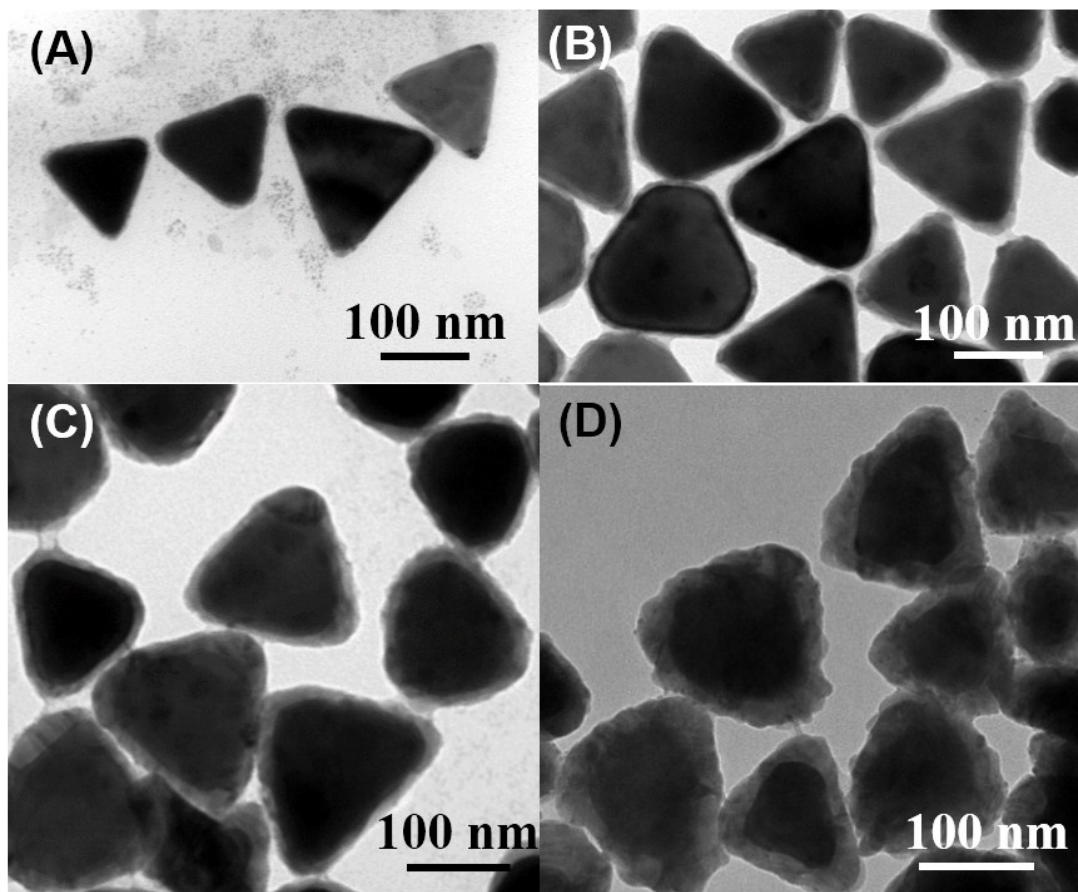


Fig. S5. Control over the thickness of the CdS shell in Ag@CdS core-shell nanoprisms by tuning the sulfuration degree of the original Ag triangular nanoprisms. The addition amount of Na_2S_x and reaction time are (A) 100 μL of Na_2S_x , 15 s, (B) 100 μL of Na_2S_x , 1 min, (C) 200 μL of Na_2S_x , 5 min, and (D) 300 μL of Na_2S_x , 5 min, respectively.

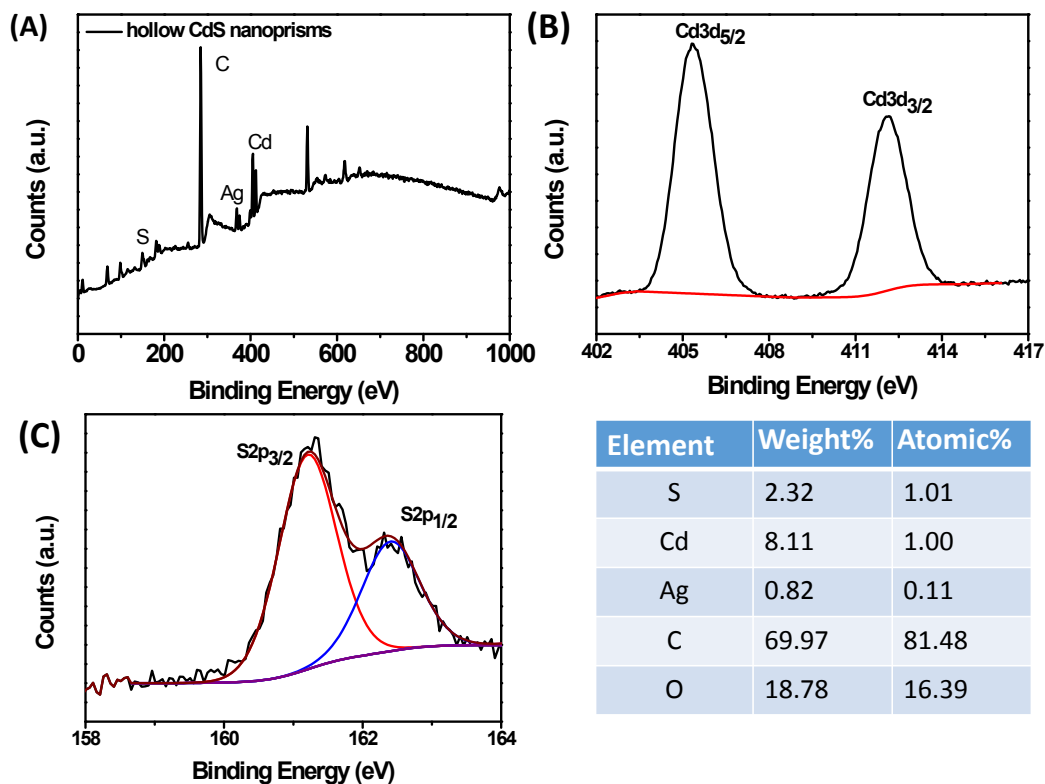


Fig. S6. (a) XPS survey spectrum and (b), (c) high-resolution XPS spectra of the hollow CdS nanoprisms. (d) Surface composition of hollow CdS nanoprisms by XPS analysis.

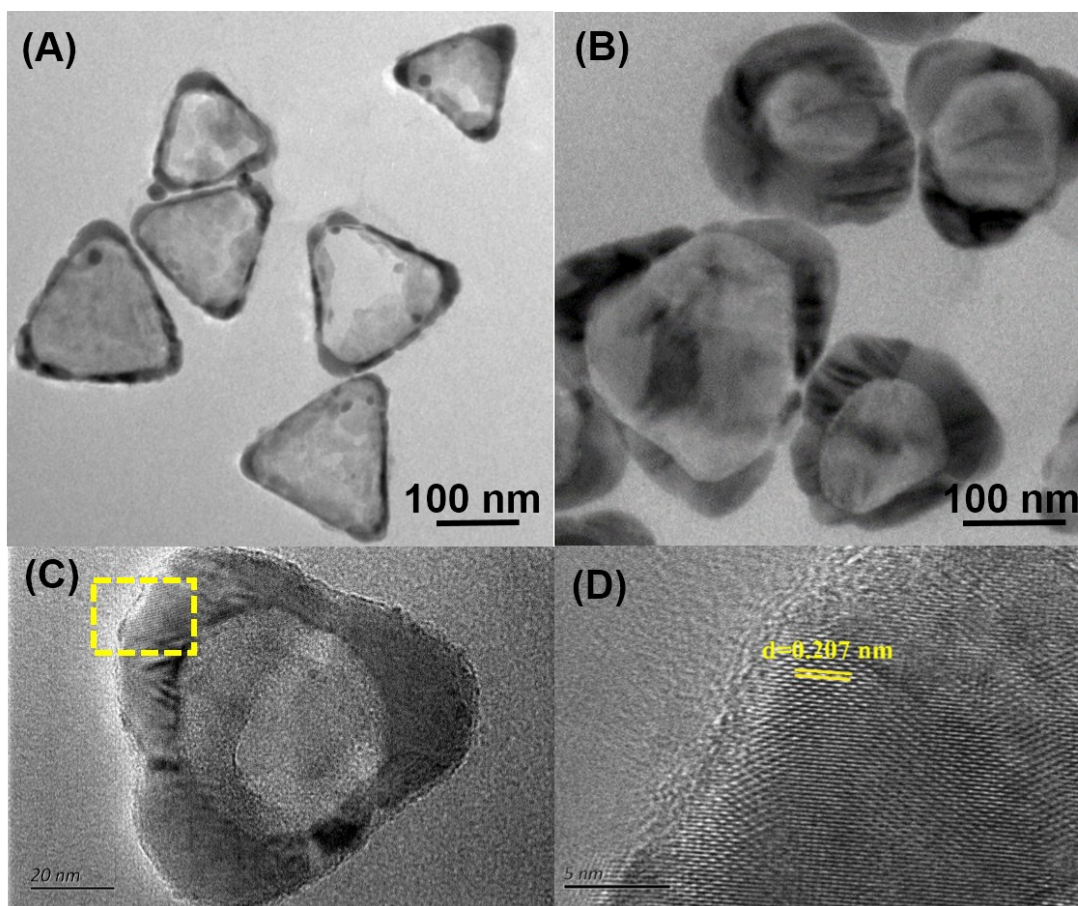


Fig. S7. Control over the thickness of the CdS shell in hollow CdS nanoprisms by tuning the sulfuration degree of the original Ag triangular nanoprisms. The addition amount of Na_2S_x and reaction time are (A) 100 μL of Na_2S_x , 1 min, (B) 200 μL of Na_2S_x , 5 min. (C, D) The HRTEM images of the samples shown in (B).

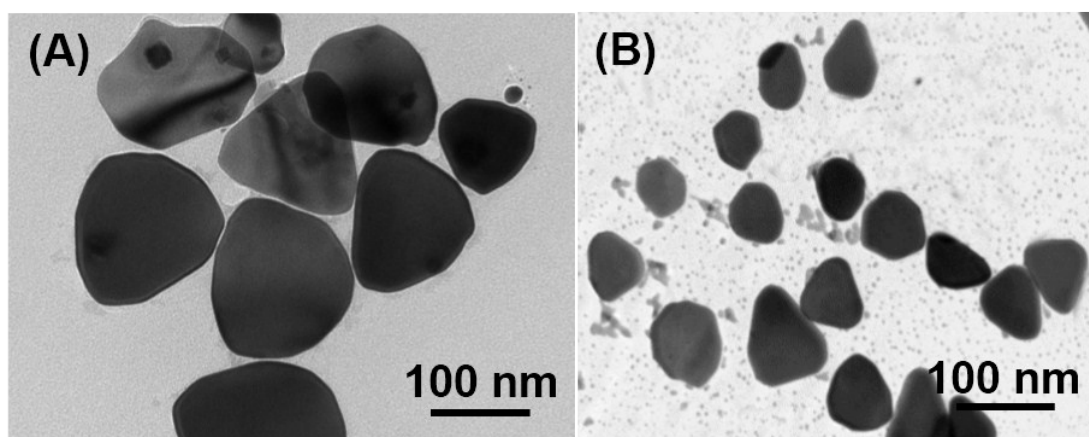


Fig. S8. TEM images of the Ag triangular nanoprisms after reacting with (A) CTAB and (B) TBP at 60 °C for 2 h, respectively. The results clearly suggest the occurrence of oxidative etching.

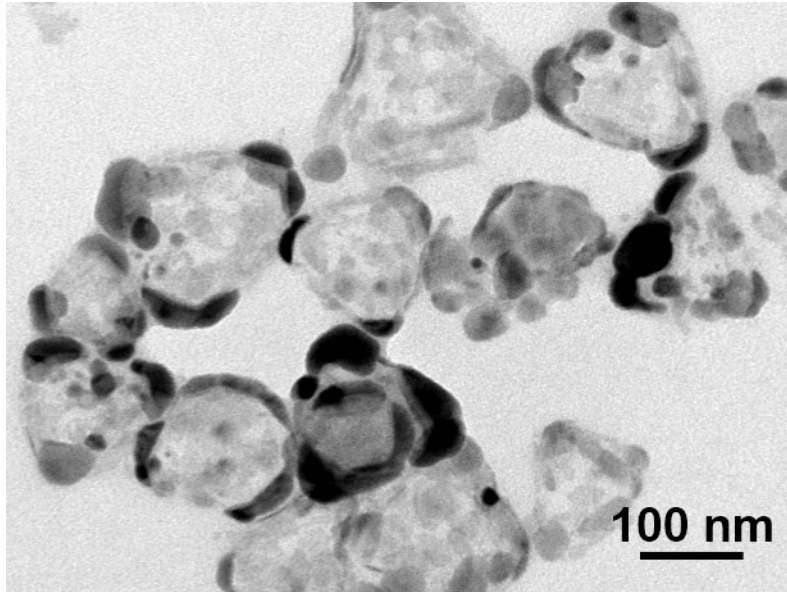


Fig. S9. TEM image of the hollow CdS nanoprisms synthesized with 50 μ L of TBP in 0.05 M CTAB aqueous solution.

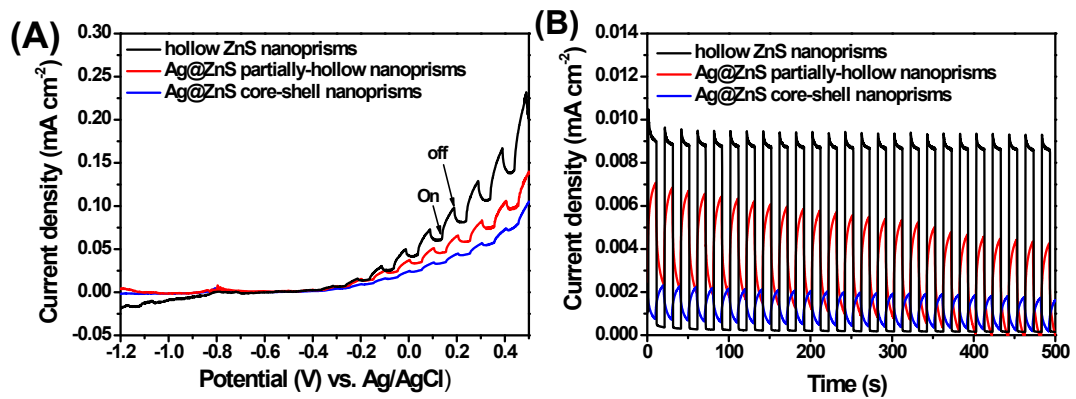


Fig. S10. (A) The photocurrent density-potential curves and (B) the photocurrent density-time curves of (at a bias of -0.2 V vs Ag/AgCl) of the different photoanodes (Ag@ZnS core-shell nanoprisms, Ag@ZnS partially-hollow nanoprisms and hollow ZnS nanoprisms) under chopped light irradiation.

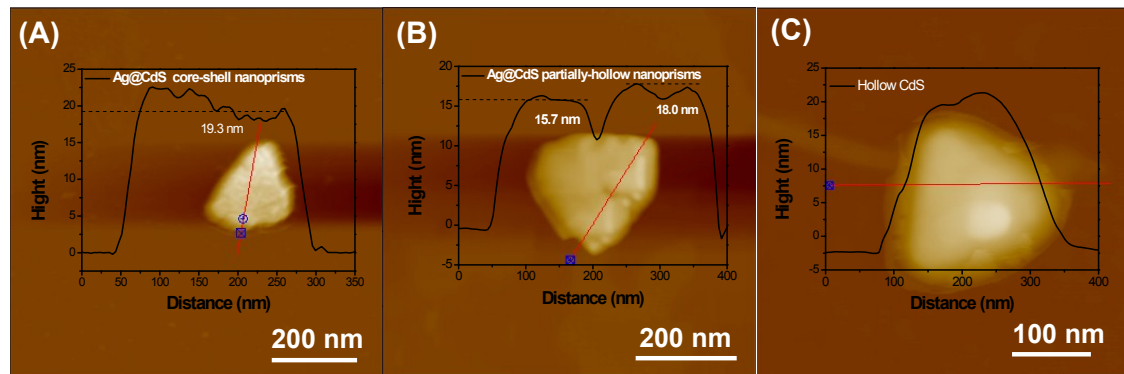


Fig. S11 The AFM images of (A) Ag@CdS core-shell nanoprisms, (B) Ag@CdS partially-hollow nanoprisms and (C) hollow CdS nanoprisms, respectively

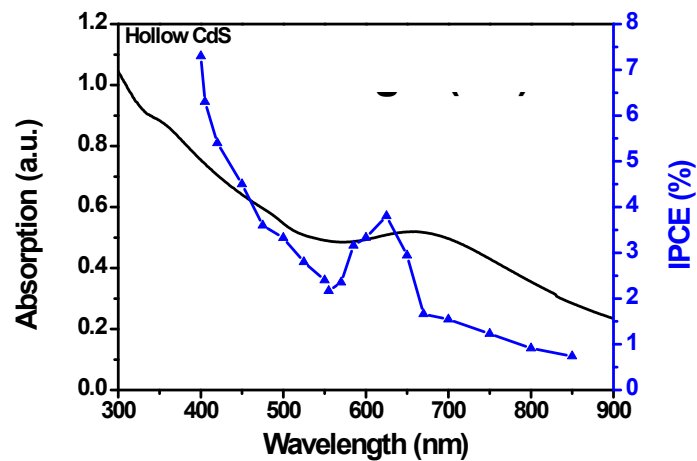


Fig.12. The absorption spectra (black) and IPCE spectrum (blue) of the hollow CdS nanoprisms photoanode. IPCE value of the photoanode measured at an applied potential of -0.4 V vs Ag/AgCl.

S1 H. M. Qian, M. Xu, X. W. Li, M. W. Ji, L. Cheng, A. Shoaib, J. J. Liu, L. Jiang, H. S. Zhu and J. T. Zhang, *Nano Res.*, 2016, **9**, 876-885.

S2 J. Zeng, J. Tao, D. Su, Y. M. Zhu, D. Qin and Y. N. Xia, *Nano Lett.*, 2011, **11**, 3010-3015.

S3 H. J. Yan, J. H. Yang, G. J. Ma, G. P. Wu, X. Zong, Z. B. Lei, J. Y. Shi, C. Li, *Journal of Catalysis*, 2009, 266, 165-168.

S4 X. Y. Cheng, J. Liu, J. W. Feng, E. H. Zhang, H. Z. Wang, X. Y. Liu, J. J. Liu, H. P. Rong, M. Xu and J. T. Zhang, *J. Mater. Chem. A*, 2018, **6**, 11898-11908.